

# The Mott insulator $\text{LaTiO}_3$ in heterostructures with $\text{SrTiO}_3$ is metallic

H. Ishida<sup>1</sup> and A. Liebsch<sup>2</sup>

<sup>1</sup>*College of Humanities and Sciences, Nihon University, and CREST JST, Tokyo 156, Japan*

<sup>2</sup>*Institut für Festkörperforschung, Forschungszentrum Jülich, 52425 Jülich, Germany*

It is shown that  $\text{LaTiO}_3$  in superlattices with  $\text{SrTiO}_3$  is not a Mott insulator but a strongly correlated metal. The tetragonal lattice geometry imposed by the  $\text{SrTiO}_3$  substrate leads to an increase of the  $\text{Ti } 3d t_{2g}$  band width and a reversal of the  $t_{2g}$  crystal field relative to the orthorhombic bulk geometry. Using dynamical mean field theory based on finite-temperature multi-band exact diagonalization we show that, as a result of these effects, local Coulomb interactions are not strong enough to induce a Mott transition in tetragonal  $\text{LaTiO}_3$ . The metallicity of these heterostructures is therefore not an interface property but stems from all  $\text{LaTiO}_3$  planes.

DOI:

PACS numbers: 73.21.-b, 71.27.+a., 73.40.-c 78.20.-e

There exists currently considerable interest in the design of nano-materials with electronic properties that differ qualitatively from those of the constituent components in their bulk form. A particularly intriguing example is the formation of a thin metallic layer at the interface between two insulators. For instance,  $\text{SrTiO}_3$  is a band insulator with an empty  $d$  band, whereas  $\text{LaTiO}_3$ , with one  $d$  electron per site, is regarded as a textbook Mott insulator because of strong local Coulomb interactions [1]. Nevertheless, the pioneering work by Ohtomo et al. [2] shows that  $\text{LaTiO}_3/\text{SrTiO}_3$  superlattices are metallic, where the overall conductivity depends on the thickness of the  $\text{LaTiO}_3$  interlayers and on the spacing between them. This phenomenon appears to follow from the fact that the Ti interface layer between adjacent La and Sr planes formally exhibits a  $3d^{0.5}$  valency, in contrast to the  $3d^1$  and  $3d^0$  configurations of bulk  $\text{LaTiO}_3$  and  $\text{SrTiO}_3$ , respectively. Other examples are  $\text{LaAlO}_3/\text{SrTiO}_3$  heterostructures where a conducting interface was observed although both constituents are wide band gap perovskite insulators [3]. Very recently, various other perovskite superlattices have been investigated experimentally [4, 5, 6, 7, 8, 9, 10, 11].

One of the hallmarks of transition metal oxides is their extreme sensitivity to small changes of key parameters such as temperature, pressure, impurity concentration, or structural distortion [1]. The aim of this work is to demonstrate that, as a result of a subtle change of crystal structure,  $\text{LaTiO}_3$  in superlattices with  $\text{SrTiO}_3$  is a strongly correlated metal, rather than a Mott insulator like bulk  $\text{LaTiO}_3$ . As a consequence, the metallicity observed in [2] is not only a property of the interface but of the entire  $\text{LaTiO}_3$  layer.

The origin of this symmetry induced insulator to metal transition is that, when  $\text{LaTiO}_3$  is grown on cubic  $\text{SrTiO}_3$ , the substrate imposes a tetragonal geometry on the first few layers [12]. As we show below, this structural modification leads to two significant changes of the electronic properties. First, it causes a substantial increase of the  $\text{Ti } t_{2g}$  band width. Second, the  $t_{2g}$  crystal field is weaker and has the opposite sign compared to bulk

$\text{LaTiO}_3$ . Both effects ensure that the Mott transition in tetragonal  $\text{LaTiO}_3$  occurs at a significantly larger critical Coulomb energy  $U_c$  than in bulk  $\text{LaTiO}_3$ . Thus, for realistic values of  $U$ , thin  $\text{LaTiO}_3$  layers in heterostructures with  $\text{SrTiO}_3$  are strongly correlated metals. These results underline the importance of carefully characterizing the interfaces of superlattices that might be employed in future devices.

The electronic properties of  $\text{LaTiO}_3/\text{SrTiO}_3$  heterostructures have been studied theoretically within a variety of single-electron and many-electron models [13, 14, 15, 16, 17, 18, 19, 20, 21]. The conditions under which  $\text{LaTiO}_3$  in these superlattices might be a Mott insulator, however, have not yet been explored. In view of the striking interplay between  $\text{Ti } 3d t_{2g}$  orbital degrees of freedom and local Coulomb interactions this issue is crucial and might differ considerably from the situation in bulk  $\text{LaTiO}_3$ . As shown by Pavarini *et al.* [22], the noncubic octahedral distortions in orthorhombic bulk  $\text{LaTiO}_3$  give rise to nondiagonal components of the  $t_{2g}$  density of states. Nevertheless, from these orbitals a new basis can be constructed (denoted here as  $a_g, e'_g$ ), in which the local density of states is nearly diagonal, and where the  $a_g$  contribution lies about 200 meV below the nearly degenerate pair of  $e'_g$  components, in qualitative agreement with experimental findings [23]. The local Coulomb energy greatly enhances this  $\text{Ti } 3d$  orbital polarization so that for  $U \approx 5$  eV a Mott transition occurs where the  $a_g$  band is nearly half-filled and the  $e'_g$  states are nearly empty [22]. The important conclusion from this picture is that the metal insulator transition in  $\text{LaTiO}_3$  is intimately connected to the sign and magnitude of the  $t_{2g}$  crystal field splitting which reflects, in turn, the orientation and magnitude of the noncubic lattice distortion.

Here we combine *ab initio* electronic structure calculations for the  $\text{SrTiO}_3$  induced tetragonal geometry of  $\text{LaTiO}_3$  with finite-temperature dynamical mean field theory (DMFT) [24, 25] and compare the correlated electronic properties with those of the bulk orthorhombic structure. As impurity solver we use a recent multi-band extension [26] of exact diagonalization (ED) [27]

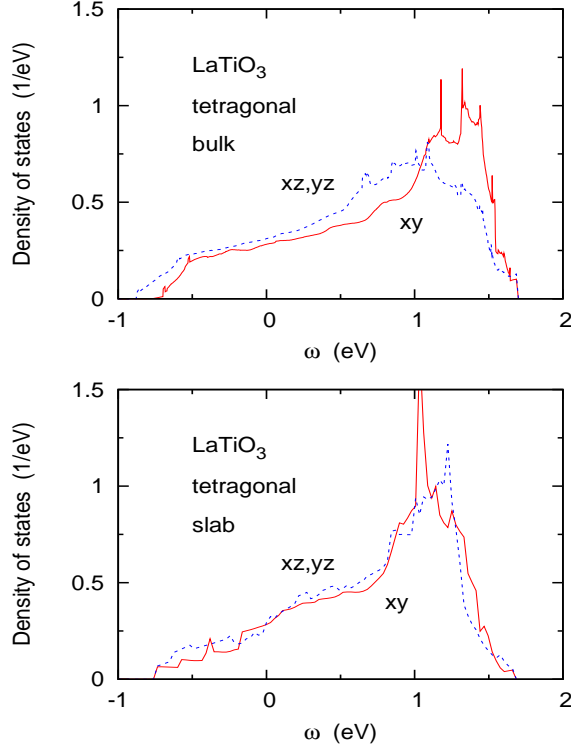


FIG. 1: (Color online) Upper panel:  $t_{2g}$  density of states components  $\text{LaTiO}_3$  in hypothetical tetragonal bulk geometry. Solid (red) curve:  $d_{xy}$  states, dashed (blue) curves:  $d_{xz,yz}$  states.  $E_F = 0$ . Lower panel: analogous density of states components for central Ti atom in  $(\text{LaTiO}_3)_6/(\text{SrTiO}_3)_4$  superlattice (see text).

which has been shown to be highly useful for the study of strong correlations in several transition metal oxides [26, 28, 29, 30]. Since this approach does not suffer from sign problems the full Hund exchange including spin-flip and pair-exchange contributions can be taken into account. Also, relatively large Coulomb energies and low temperatures can be reached.

The structures of  $\text{LaTiO}_3$  in the tetragonal bulk and superlattice geometries were optimized via the Vienna Ab-initio Simulation Package (VASP) [31], an implementation of the projector augmented-wave method [32], where the total energy of the system was calculated within non-spin-polarized GGA. The in-plane lattice constant was fixed to that of  $\text{SrTiO}_3$ ,  $a = b = 3.92 \text{ \AA}$ , whereas the lattice parameters in the  $z$  direction were fully optimized. We assumed a  $1 \times 1$  geometry without considering rotation and tilting of  $\text{TiO}_6$  octahedra. For each optimized geometry, we performed an LDA calculation using a home-made FLAPW code to calculate the partial density of states projected on Ti  $3d$  orbitals in muffin-tin spheres. For the bulk structure, the  $z$  axis layer spacing  $c = 4.01 \text{ \AA}$  is only slightly smaller than  $c = 4.106 \text{ \AA}$  obtained for a tetragonal lattice with the same unit cell volume as in the orthorhombic case.

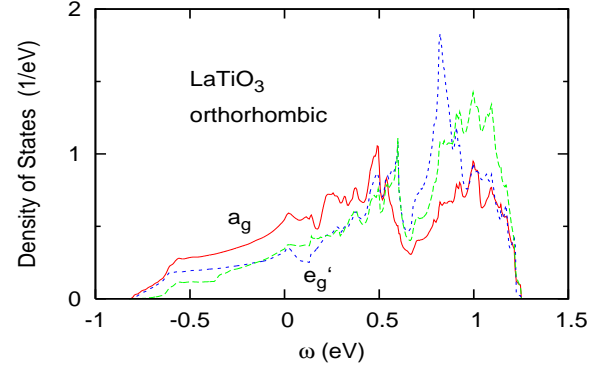


FIG. 2: (Color online) Density of states components of orthorhombic bulk  $\text{LaTiO}_3$  in nearly diagonal subband representation [22]. Solid (red) curve:  $a_g$  states, dashed (blue and green) curves:  $e'_g$  states.  $E_F = 0$ .

Fig. 1 shows the Ti  $t_{2g}$  density of states components for the hypothetical tetragonal bulk geometry of  $\text{LaTiO}_3$  (upper panel). In this symmetry, the singly degenerate  $d_{xy}$  density differs from the doubly degenerate  $d_{xz,yz}$  densities. In the experimental work of Ohtomo *et al.* [2], rather thin  $\text{LaTiO}_3$  layers containing up to five La planes were studied. The lower panel of Fig. 1 shows the  $t_{2g}$  density of states components for a  $(\text{LaTiO}_3)_6/(\text{SrTiO}_3)_4$  superlattice, containing five Ti layers in a nominal  $d^1$  configuration (only La neighboring planes), three  $d^0$  Ti layers (only Sr neighboring planes), and two  $d^{0.5}$  Ti interface layers (La and Sr neighboring planes). Plotted is the density of states for the central Ti atom within the  $\text{LaTiO}_3$  slab. The vertical height of the  $\text{O}_6$  octahedron surrounding this atom,  $3.98 \text{ \AA}$ , is slightly smaller than that in the tetragonal bulk,  $4.01 \text{ \AA}$ . As a result, the difference between the  $d_{xy}$  and  $d_{xz,yz}$  densities is even smaller than that in bulk case shown in the upper panel of Fig. 1.

The overall width of the  $t_{2g}$  bands for both tetragonal structures is about  $W_{\text{tetra}} \approx 2.5 \text{ eV}$ , where we have neglected small additional spectral weight in the region of the empty  $e_g$  bands at higher energies. Also, the centroid of the singly degenerate  $d_{xy}$  band is seen to lie above that of the  $d_{xz,yz}$  bands. As a result of this *positive* crystal field splitting, the subband occupancies (per spin band) are  $n_{xy} \approx 0.14$ ,  $n_{xz,yz} \approx 0.18$  for the tetragonal bulk and  $n_{xy} \approx 0.15$ ,  $n_{xz,yz} \approx 0.175$  for the tetragonal slab.

For comparison we show in Fig. 2 the  $a_g$  and  $e'_g$  densities of orthorhombic bulk  $\text{LaTiO}_3$  [22] which are obtained from a linear transformation of the original Ti  $d_{xy,xz,yz}$  orbitals. As mentioned above, in the  $a_g, e'_g$  basis the orthorhombic density of states is nearly diagonal and the centroid of the  $a_g$  density lies about 200 meV below the two  $e'_g$  components, implying a *negative* crystal field splitting between the singly and doubly degenerate densities. The subband occupancies (per spin band) are  $n_{a_g} \approx 0.23$  and  $n_{e'_g} \approx 0.135$ . Thus, orbital po-

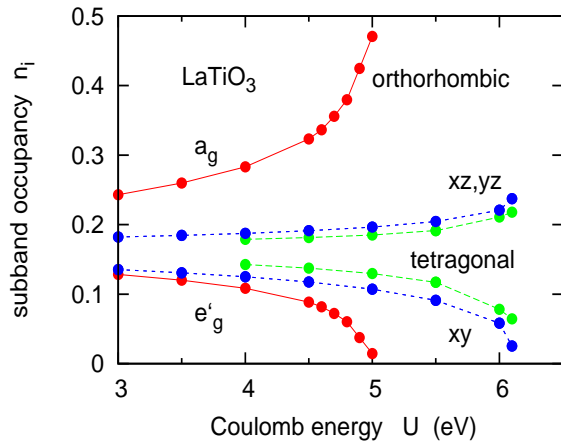


FIG. 3: (Color online) Ti 3d subband occupancies of LaTiO<sub>3</sub> as a function of local Coulomb energy. Solid (red) curves: orthorhombic bulk geometry, indicating metal insulator transition at  $U \approx 5$  eV. Short-dashed (blue) curves: tetragonal bulk geometry, long-dashed (green) curves: tetragonal slab geometry, both indicating Mott transitions at  $U > 6$  eV. Since the crystal field splitting has opposite sign in the orthorhombic and tetragonal structures, the orbital polarization between singly degenerate  $a_g$  ( $d_{xy}$ ) and doubly degenerate  $e'_g$  ( $d_{xz,yz}$ ) states is reversed.

larization is much larger than for the tetragonal structures shown in Fig. 1 and has the opposite sign. Moreover, the width of the  $a_g$ ,  $e'_g$  bands,  $W_{\text{ortho}} \approx 2$  eV, is considerably smaller than in the tetragonal case. On the whole, therefore, the noncubic distortions are significantly smaller for the tetragonal interlayer structure than for the orthorhombic bulk form of LaTiO<sub>3</sub>. This difference is also apparent in the shape of the density of states since the tetragonal distributions shown in Fig. 1 resemble more closely the characteristic  $t_{2g}$  density of cubic SrVO<sub>3</sub> (width  $W_{\text{cubic}} = 2.8$  eV [22]).

We now show that the combined influence of these differences: the wider band width, the weaker orbital polarization, and the opposite sign of this polarization, implies that LaTiO<sub>3</sub> in the tetragonal superlattice geometry is a strongly correlated metal, rather than a Mott insulator as in its orthorhombic bulk form.

To evaluate the electronic properties of LaTiO<sub>3</sub> in the presence of strong local Coulomb interactions we use multi-band ED/DMFT [26]. Full Hund exchange is included, with the exchange energy  $J = 0.65$  eV held fixed at the value appropriate for the bulk material [22]. To locate the Mott transition, the intra-orbital Coulomb energy  $U$  is varied, and the inter-orbital Coulomb interaction is given by  $U' = U - 2J$ . The temperature is  $T = 20$  meV.

Fig. 3 shows the  $a_g$ ,  $e'_g$  subband occupancies as a function of Coulomb energy. For the orthorhombic geometry, nearly complete orbital polarization is reached at about  $U = 5$  eV, which agrees with previous DMFT re-

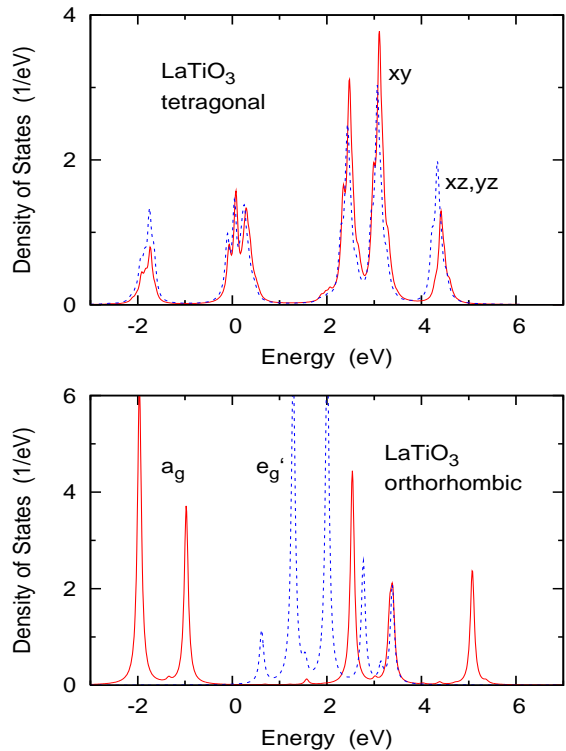


FIG. 4: (Color online) LaTiO<sub>3</sub> 3d  $t_{2g}$  spectral distributions. Upper panel: tetragonal superlattice geometry,  $U = 5.5$  eV, indicating strongly correlated metallic behavior. Lower panel: orthorhombic bulk geometry,  $U = 5$  eV, indicating Mott insulating behavior. Solid (red) curves: singly degenerate  $d_{xy}$  ( $a_g$ ) states, dashed (blue) curves: doubly degenerate  $d_{xz,yz}$  ( $e'_g$ ) states;  $E_F = 0$ .

sults using the Quantum Monte Carlo technique as impurity solver [22]. The spectral distributions (see Fig. 4) show that the nearly half-filled  $a_g$  band then consists of lower and upper Hubbard peaks whereas the  $e'_g$  bands are pushed above the Fermi level [22, 30]. In the case of the tetragonal structures, the situation is qualitatively different since the crystal field is weaker and has opposite sign. Now the enhancement of the orbital polarization via the Coulomb interaction implies that the  $d_{xy}$  band is pushed above the Fermi level and that the degenerate  $d_{xz,yz}$  bands are driven to 1/4 occupancy. As a result of this reversal of crystal field, and because of its weaker magnitude (i.e., weaker orbital polarization in the uncorrelated limit), the metal insulator transition occurs above  $U = 6$  eV. Since the local Coulomb energy for Ti is approximately 5 eV [22], this result implies that in the tetragonal geometry LaTiO<sub>3</sub> is on the metallic side of the Mott transition. As mentioned above, we have neglected small contributions to the tetragonal density of states in the region of the empty  $e_g$  bands. Inclusion of these states would increase the tetragonal  $t_{2g}$  band width and reinforce the metallic behavior.

As can be seen in Fig. 3, the Mott transition for the

tetragonal slab geometry occurs at slightly larger  $U$  than for the tetragonal bulk. This shift is a consequence of the smaller orbital polarization in the former case, associated with the weaker deviations of the density of states components from cubic symmetry, as is evident also from the results shown Fig. 1.

In Fig. 4 we compare the  $\text{LaTiO}_3$   $t_{2g}$  spectral distributions for the tetragonal slab and orthorhombic bulk crystal structures. Since we are concerned here only with the difference between metallic and insulating behavior, it is sufficient to use the ED cluster spectra which can be evaluated at real  $\omega$ , without requiring extrapolation from imaginary Matsubara frequencies. In the orthorhombic case, the system is already insulating at  $U = 5$  eV, with an excitation gap formed between the lower Hubbard peak of the  $a_g$  band and the empty  $e'_g$  bands, in agreement with Ref. [22]. The tetragonal slab geometry, on the other hand, is still metallic at  $U = 5.5$  eV, with conduction states near  $E_F$  from  $d_{xy}$  and  $d_{xz,yz}$  bands.

In the DMFT calculations discussed above we have focused on the central Ti plane in the tetragonal  $\text{LaTiO}_3$  layer. Ti planes at the interface with  $\text{SrTiO}_3$  are also metallic because of the nominal  $3d^{0.5}$  occupancy [2, 13]. The mutual enhancement of both effects ensures that the entire  $\text{LaTiO}_3$  layer is metallic.

The above results demonstrate the extreme sensitivity of the electronic properties of perovskites to small changes in key parameters. In the present case, the slightly modified crystal structure caused by the deposition of  $\text{LaTiO}_3$  onto  $\text{SrTiO}_3$  gives rise to a subtle, but important change in its single-electron spectral distribution, which, in turn, has a profound effect on the properties of the correlated electron system. For an adequate interpretation of experimental data it is therefore of great importance to have accurate structural information. On the theoretical side, it is crucial to include the full details of the single-particle electronic properties for a given lattice geometry and to account for the orbital degrees of freedom in the multi-band many-body calculation.

In summary, we have shown that in  $\text{LaTiO}_3/\text{SrTiO}_3$  superlattices the change from orthorhombic to tetragonal crystal structure enforced by the  $\text{SrTiO}_3$  substrate causes a fundamental change in the electronic properties of  $\text{LaTiO}_3$ . Instead of being a Mott insulator as in the bulk geometry, it is now a highly correlated metal. Thus, the metallicity observed in these heterostructures is not only associated with the interfaces but with the entire  $\text{LaTiO}_3$  layers. It would be very interesting to use transmission electron microscopy to determine the  $\text{LaTiO}_3$  layer thickness at which the orthorhombic structure begins to be energetically favorable. Mott insulating behavior should then emerge in the central regions of these  $\text{LaTiO}_3$  layers at sufficiently large thickness.

- [2] A. Ohtomo, D.A. Muller, J.L. Grazul and H.Y. Hwang, *Nature* **419**, 378 (2002).
- [3] A. Ohtomo and H.Y. Hwang, *Nature* **427**, 423 (2004).
- [4] M. Takizawa *et al.*, *Phys. Rev. Lett.* **97**, 057601 (2006).
- [5] L.F. Kourkoutis *et al.*, *Phys. Rev. Lett.* **97**, 256803 (2006).
- [6] K. Maekawa *et al.*, *Phys. Rev. B* **76**, 115121 (2007).
- [7] H. Wadati *et al.*, arXiv:0704.1837.
- [8] S.J. May *et al.*, arXiv:0709.1715.
- [9] A. Bhattacharya *et al.*, arXiv:0710.1452.
- [10] Y. Hotta, T. Susaki and H. Y. Hwang, arXiv:0710.2174.
- [11] W.C. Sheets, B. Mercey and W. Prellier, arXiv:0710.2476.
- [12] K.H. Kim *et al.*, *Phys. Stat. Solidi A* **200**, 346 (2003).
- [13] S. Okamoto and A.J. Millis, *Nature* **427**, 630 (2004); *Phys. Rev. B* **70**, 075101 (2004); *ibid.* **70**, 241104(R) (2004); *ibid.* **72**, 235108 (2005).
- [14] J.K. Freericks, *Phys. Rev. B* **70**, 195342 (2004).
- [15] Z.S. Popovic and S. Satpathy, *Phys. Rev. Lett.* **94**, 176805 (2005).
- [16] S. Okamoto, A.J. Millis and N.A. Spaldin, *Phys. Rev. Lett.* **97**, 056802 (2006).
- [17] D.R. Hamann, D.A. Muller and H.Y. Hwang, *Phys. Rev. B* **73**, 195403 (2006).
- [18] W.-C. Lee and A.H. MacDonald, *Phys. Rev. B* **74**, 075106 (2006); cond-mat/0708.0554.
- [19] S.S. Kancharla and E. Dagotto, *Phys. Rev. B* **74**, 195427 (2006).
- [20] R. Pentcheva and W.E. Pickett, *Phys. Rev. Lett.* **98**, 016802 (2007).
- [21] A. Rüegg, S. Pilgram and M. Sigrist, cond-mat/0701642.
- [22] E. Pavarini, S. Biermann, A. Poteryaev, A.I. Lichtenstein, A. Georges and O.K. Andersen, *Phys. Rev. Lett.* **92**, 176403 (2004); E. Pavarini, A. Yamasaki, J. Nuss, and O.K. Andersen, *New J. Phys.* **7**, 188 (2005).
- [23] M. Cwik *et al.*, *Phys. Rev. B* **68**, 060401 (2003); J. Hemberger *et al.*, *Phys. Rev. Lett.* **91**, 066403 (2003); H.W. Haverkort *et al.*, *ibid.* **94**, 056401 (2005).
- [24] W. Metzner and D. Vollhardt, *Phys. Rev. Lett.* **62**, 324 (1989); E. Müller-Hartmann, *Z. Phys. B* **74**, 507 (1989); A. Georges and G. Kotliar, *Phys. Rev. Lett.* **45**, 6479 (1992); M. Jarrel, *Phys. Rev. Lett.* **69**, 168 (1992).
- [25] A. Georges, G. Kotliar, W. Krauth and M.J. Rozenberg, *Rev. Mod. Phys.* **68**, 13 (1996).
- [26] C.A. Perroni, H. Ishida and A. Liebsch, *Phys. Rev. B* **75**, 045125 (2007). See also: A. Liebsch, *Phys. Rev. Lett.* **95**, 116402 (2005); A. Liebsch and T. A. Costi, *Eur. Phys. J.* **51**, 523 (2006).
- [27] M. Caffarel and W. Krauth, *Phys. Rev. Lett.* **72**, 1545 (1994).
- [28] A. Liebsch and H. Ishida, *Phys. Rev. Lett.* **98**, 216403 (2007).
- [29] H. Ishida and A. Liebsch, cond-mat/0705.3627.
- [30] A. Liebsch, cond-mat/0707.1828.
- [31] G. Kresse and J. Furthmüller, *Comput. Mat. Sci.* **6**, 15 (1996) and Refs. herein.
- [32] P.E. Blöchl, *Phys. Rev. B* **50**, 17953 (1994).